Supplemental Figure 1

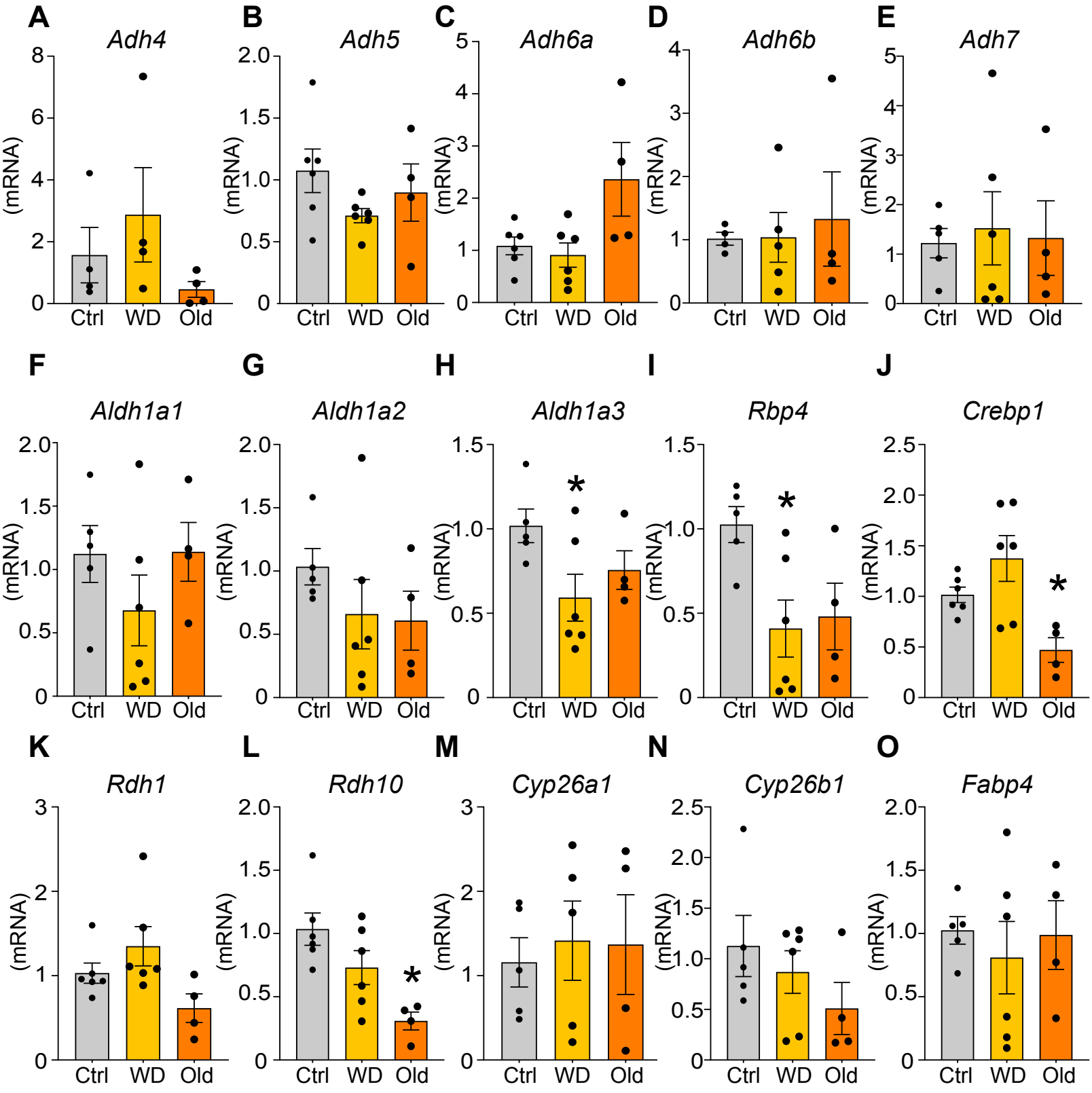

Supplemental Figure 1: Gene expression analysis of retinol metabolism pathway components in paracardial fat. (A-O) mRNA expression levels of indicated genes in paracardial fat (pCF) of control (Ctrl), western diet fed (WD) or aged (Old) wild-type mice as determined by qPCR. *n* = 4-6 per genotype. Data are represented as mean ± SEM, and data were analyzed by 1-way ANOVA with Tukey HSD Multiple Comparison tests comparing means of WD or Old mice to means of the control group. Asterisks (*) indicates significance at the alpha = 0.05 level.

Supplemental Figure 2

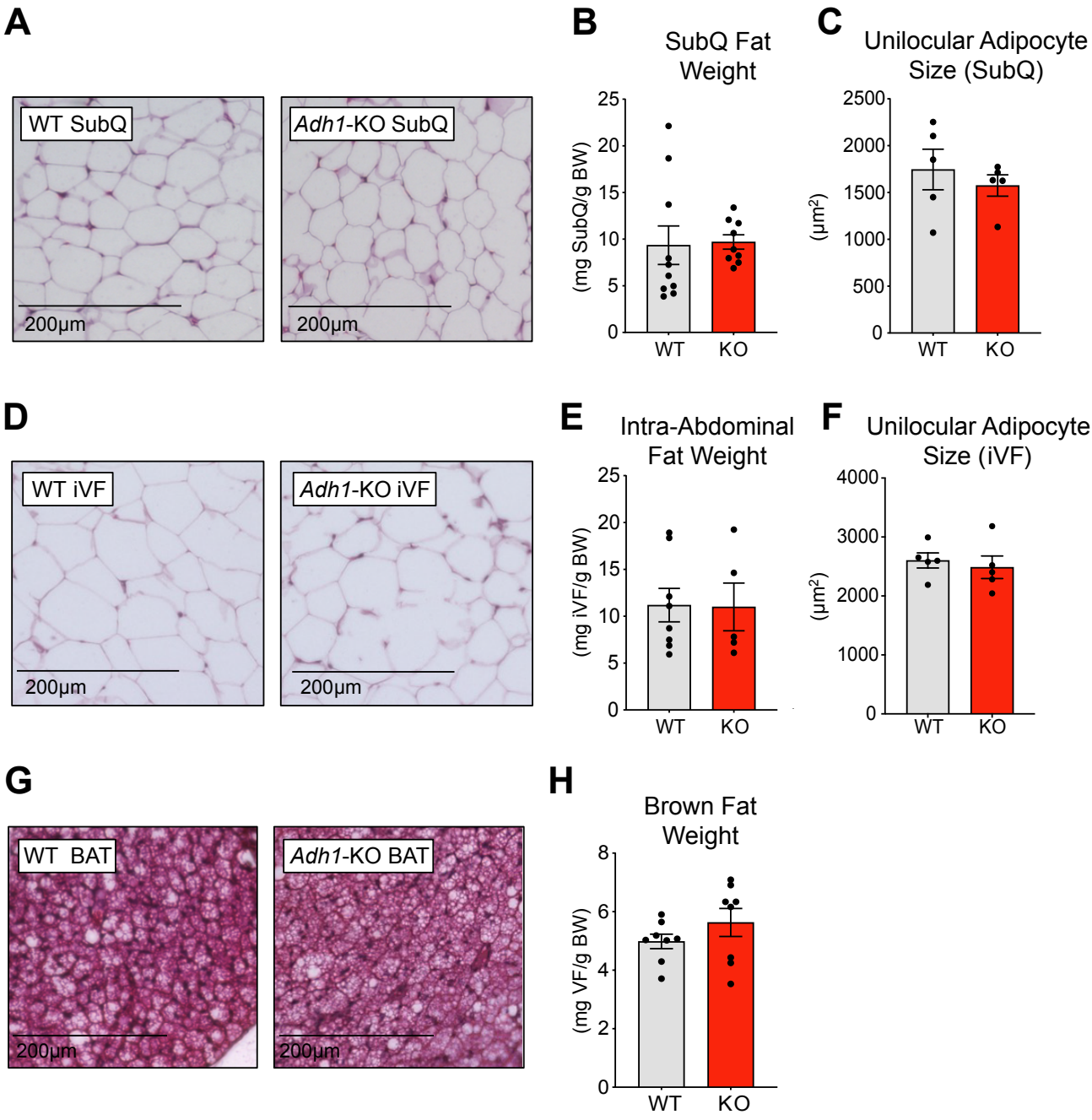

Supplemental Figure 2: The loss of *Adh1* does not affect subcutaneous, intra-abdominal or brown fat depots. (A) Representative hematoxylin and eosin (H&E) images, (B) weight and (C) unilocular adipocyte size of WT and *Adh1*-KO subcutaneous fat (SubQ). (D) Representative H&E images, (E) weight and (F) unilocular adipocyte size of WT and *Adh1*-KO intra-abdominal visceral fat (iVF). (G) Representative H&E images and (H) weight of WT and *Adh1*-KO brown fat (BAT). *n* = 5-10 per group for biological animal replicates. Data are represented as mean ± SEM, and data were analyzed by Student's t.test. Significance at the alpha = 0.05 level.

Supplemental Figure 3

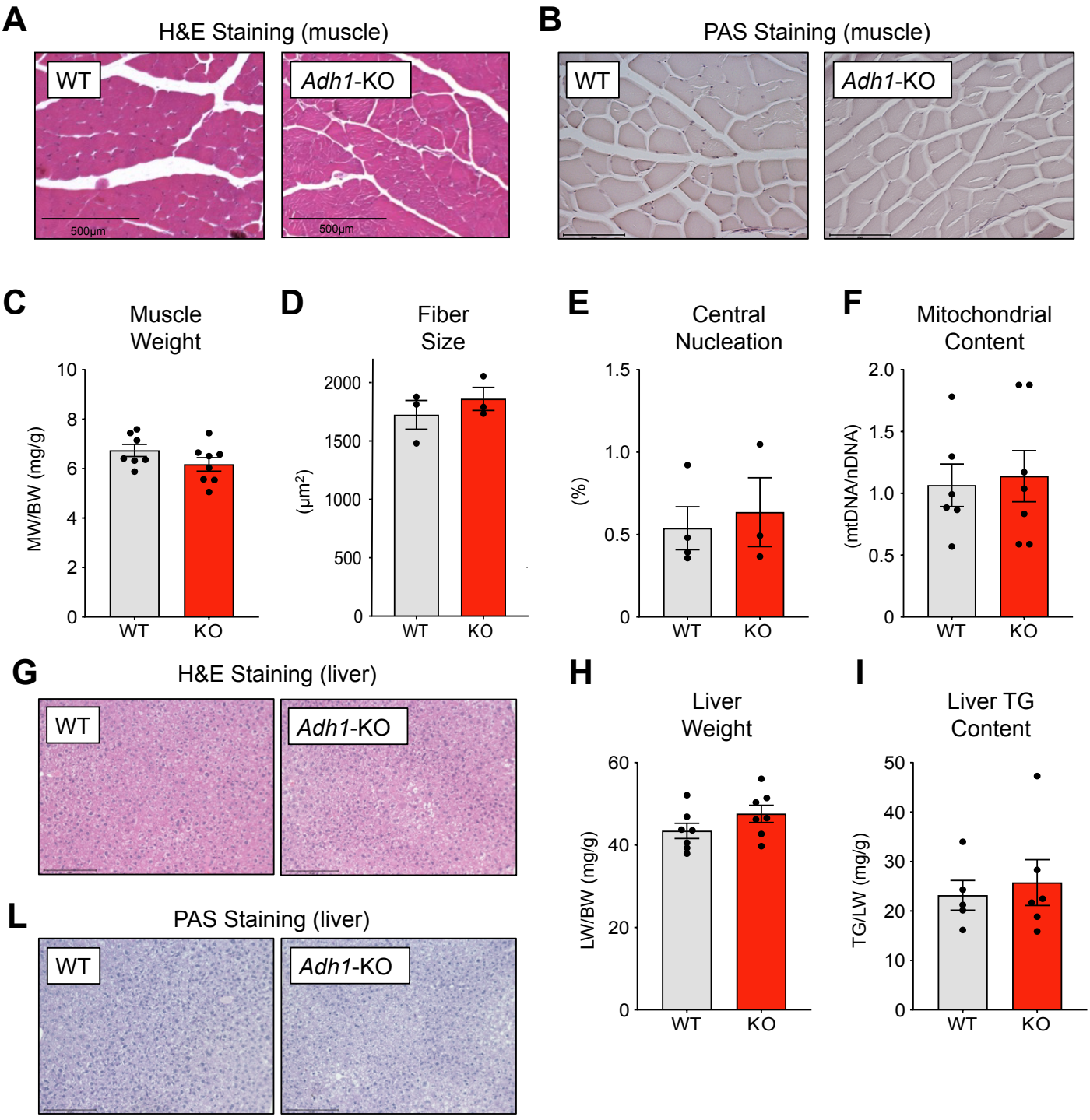

Supplemental Figure 3: The loss of *Adh1* does not affect skeletal muscle or liver.(A and B, G and L) Representative hematoxylin and eosin (H&E) (A) and periodic acid- schiff (PAS) (B) images of WT and *Adh1*-KO (KO) skeletal muscles (quadriceps) or livers. (C) Skeletal muscle weight (MW) normalized to body weight (BW), (D) fiber size, and (E) central nucleation in WT and KO quadriceps. (F) qPCR quantification of relative mitochondrial DNA (mtDNA) abundance in WT and KO skeletal muscle, normalized to nuclear DNA (nDNA) content. (H) Liver muscle weight (LW) normalized to body weight (BW). (I) Liver triglyceride (TG) content normalized to liver weight (LW). *n* = 3-7 per group for biological animal replicates. Data are represented as mean ± SEM, and data were analyzed by Student's Significance at the alpha = 0.05 level.

Supplemental Figure 4

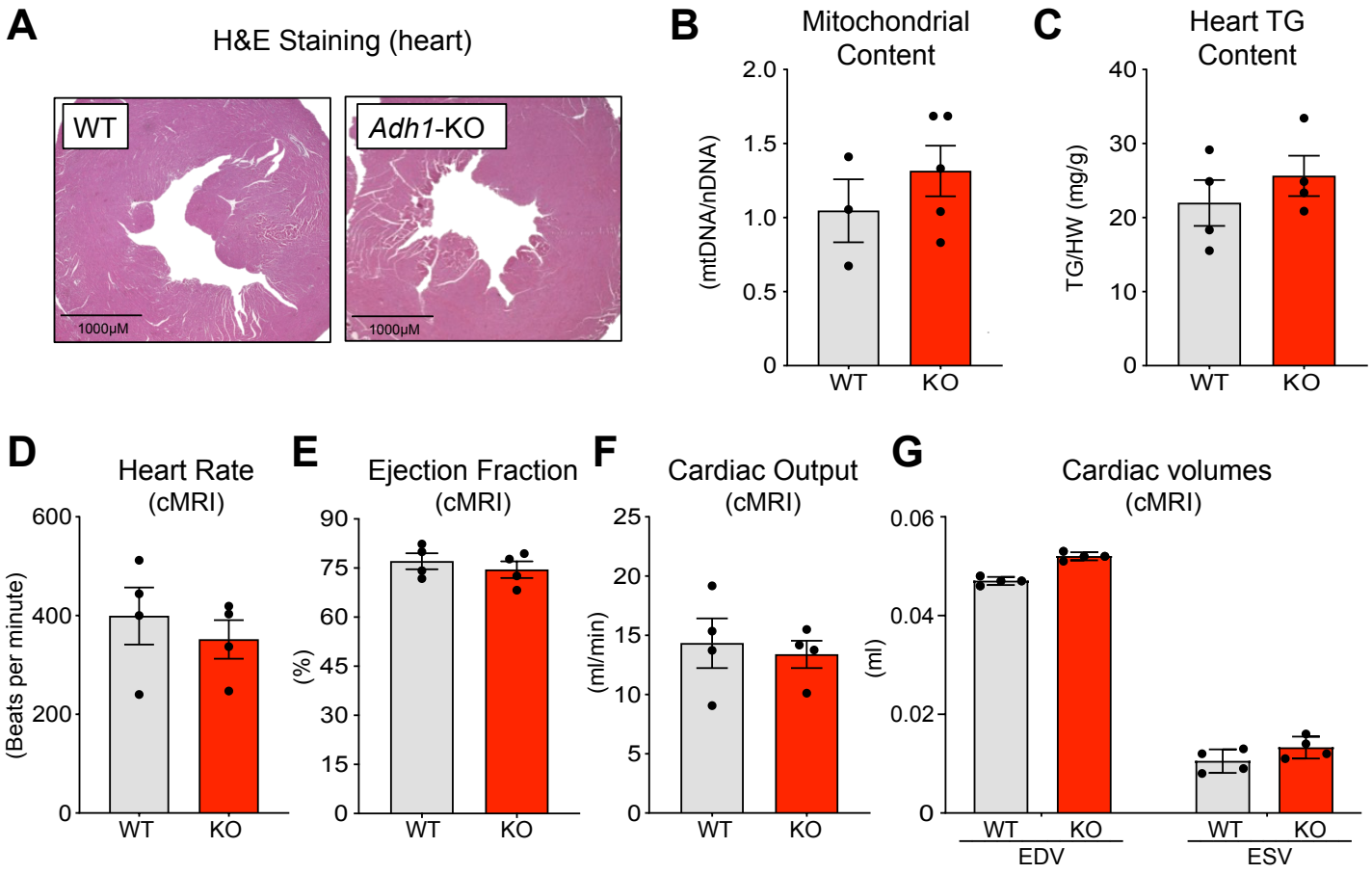

Supplemental Figure 4: The loss of *Adh1* does not affect the heart. (A) Representative hematoxylin and eosin (H&E) images of WT and *Adh1*-KO heart. (B) qPCR quantification of relative mitochondrial DNA (mtDNA) abundance in WT and *Adh1*-KO heart, normalized to nuclear DNA (nDNA) content. (C) Heart triglyceride (TG) content normalized to heart weight (HW). (D-G) Cardiac magnetic resonance imaging (cMRI) in WT and *Adh1*-KO mice for the indicated measurements. EDV=End Diastolic Volume; ESV=End Systolic Volume. *n* = 3-5 per group for biological animal replicates. Data are represented as mean ± SEM, and data were analyzed by Student's t.test. Signifigance at the alpha = 0.05 level.

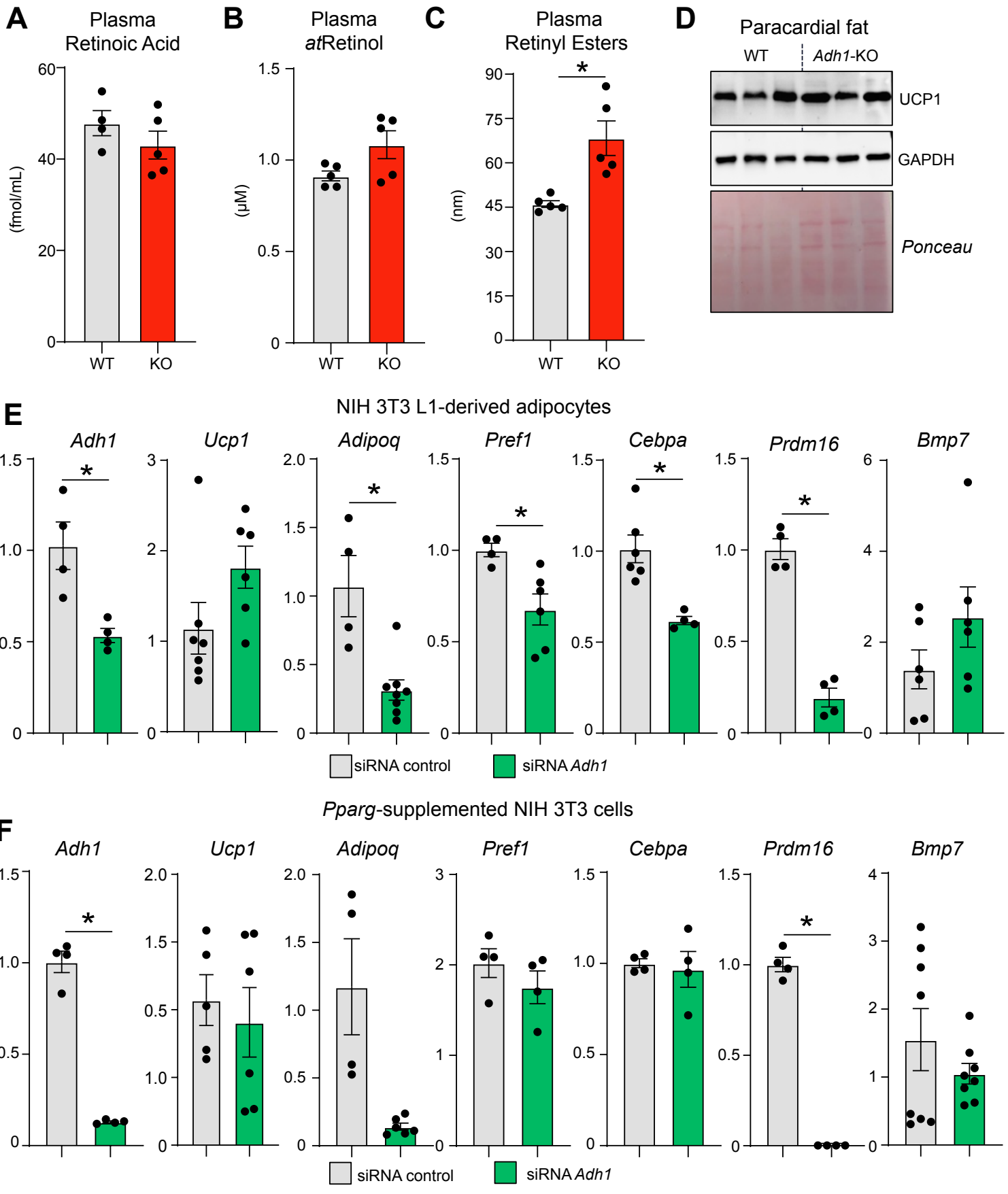

Supplemental Figure 5: Altered retinol pathway with loss of *Adh1* is *Ucp1* independent. (A) Mass spectrometry quantification of retinoic acid levels in WT and *Adh1*-KO plasma. (B- C) HPLC quantification of all trans (at) retinol and retinyl esters in WT and *Adh1*-KO plasma. (D) Western blot for the indicated proteins in WT and *Adh1*-KO paracardial fat. (E-F) qPCR quantification for the indicated genes in NIH 3T3 L1 differentiated into adipocytes (D) and NIH 3T3 supplemented with *Pparg* (E) and treated with siRNA control or siRNA against *Adh1*. *n* =4-8 per group. Data are represented as mean ± SEM, and data were analyzed by Student's t.test. Asterisks (*) indicates significance at the alpha = 0.05 level.

Supplemental Figure 6

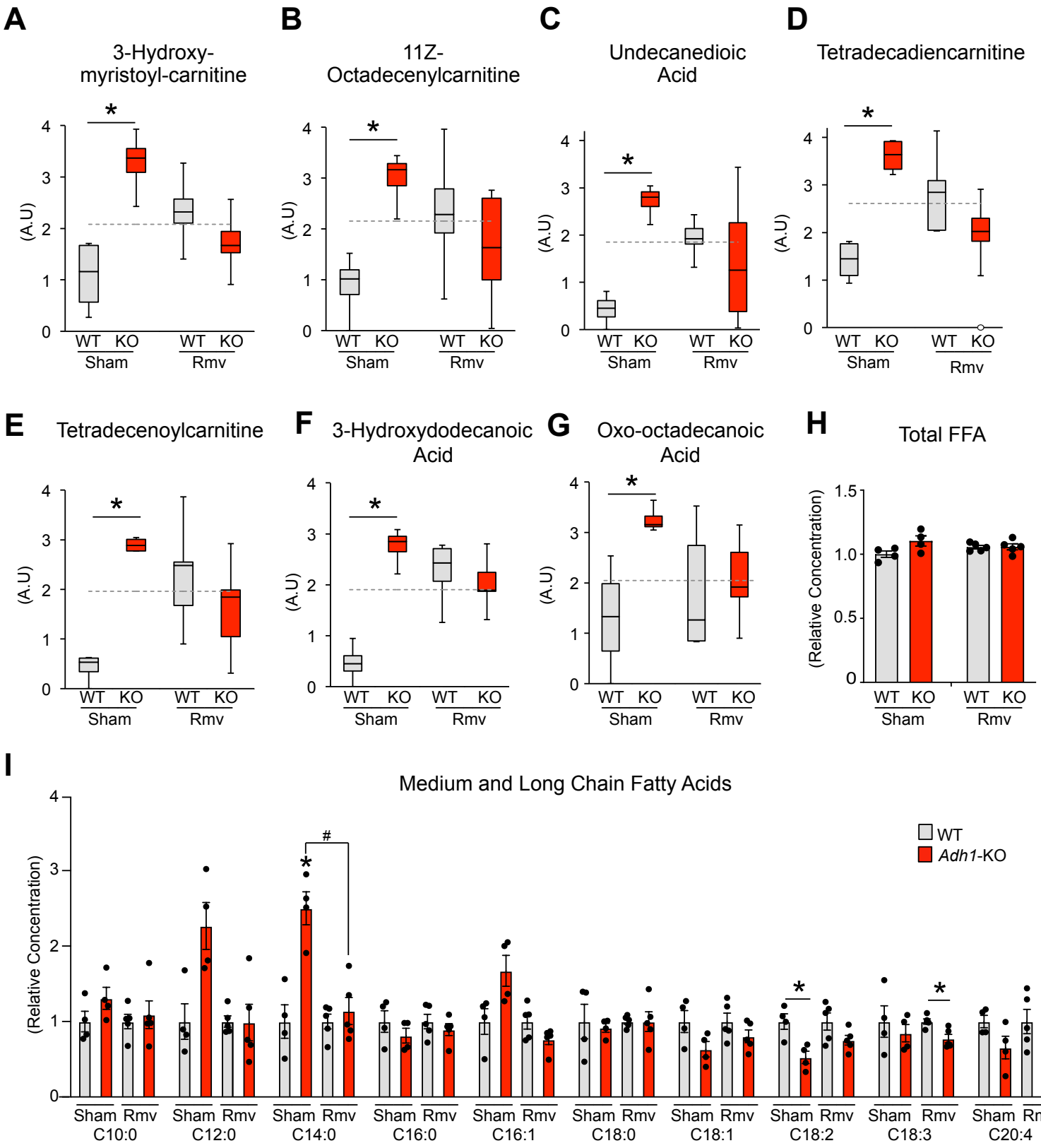

Supplemental Figure 6: Removal of paracardial fat rescues circulating metabolite and fatty acid alterations in *Adh1*-KO mice. (A-G) Relative plasma amounts for the indicated metabolites following sham or pCF removal (Rmv) surgeries. (H) Total free fatty acids (FFA) and (I) fatty acid concentration of various carbon chain length following sham or pCF removal (Rmv) surgeries. C=carbon. Values are normalized to WT condition. *n* = 4-5 biological replicates per group. Data are represented as box plotsor by mean ± SEM. Data were analyzed by 2-way ANOVA with Tukey HSD Multiple Comparison tests comparing means of all groups. Asterisks (*) indicates significance at the alpha = 0.05 level between WT and KO animals of the same treatment groups, hash (#) indicates significance at the alpha = 0.05 between genotypes.

Supplemental Figure 7

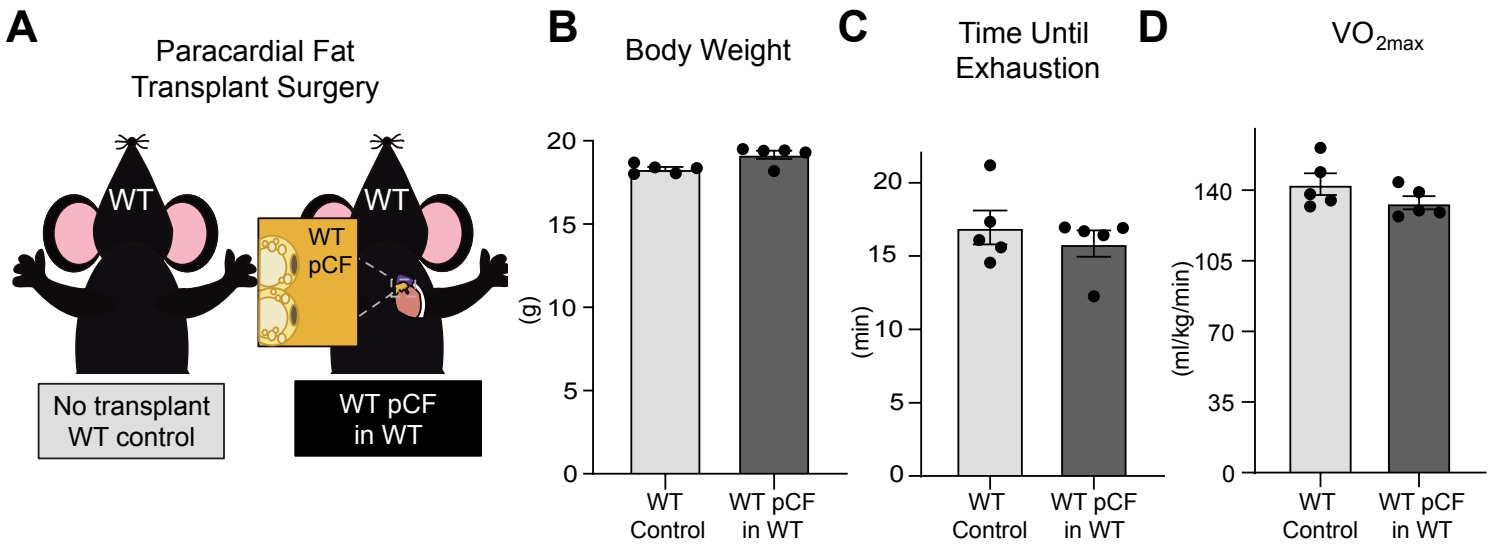

Supplemental Figure 7: Transplant of healthy paracardial fat does not affect wild type mice. (A) Schematics of paracardial fat (pCF) transplant surgery. (B) Body weight in no transplant wild type controls (WT control) and WT mice receiving WT pCF to replace their endogenous pCF (WT pCF in WT). (C) Time until exhaustion, and (D) Maximal oxygen consumption (VO_{2max}) in the indicated group of mice subjected to maximal exercise test. *n* = 5 animals group for biological animal replicates. Data are represented as mean ± SEM, and data were analyzed by Student's t.test. Significance at the alpha = 0.05 level.

Supplemental Figure 8

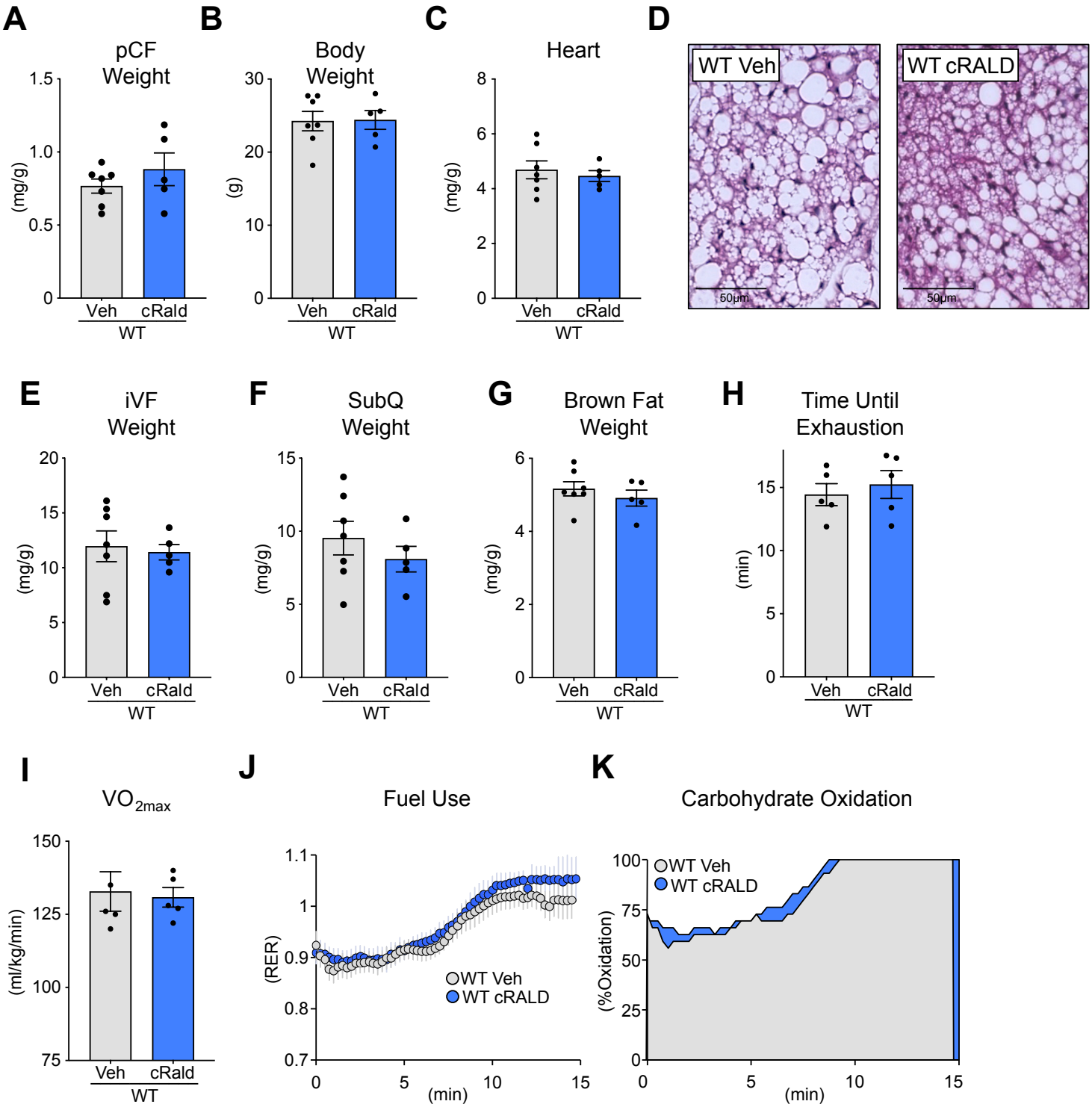

Supplemental Figure 8: Chronic Rald treatment does not affect healthy wild type mice. (A-C) pCF weight normalized to body weight, body weight and heart weight normalized to body weight for the indicated treatments. Veh=vehicle; cRald=chronic Rald. (B) Representative H&E images of pCF from the indicated treatments. (E-G) Intra-abdominal visceral fat (iVF), Subcutaneous (SubQ) and Brown Fat weight normalized to body weight following the indicated treatments. (H) Time until exhaustion, (I) Maximal oxygen consumption (VO_{2max}), (J) respiratory exchange ratio (RER) and (K) carbohydrate oxidation for the indicated treatments in wild type mice subjected to maximal exercise test. *n* = 4-7 animals group for biological animal replicates. Data are represented as mean ± SEM, and data were analyzed by Student's t.test. Significance at the alpha = 0.05 level.

Supplemental Material and Methods.

Paracardial fat removal and transplant study: Anesthetized animals were fist subjected to endotracheal intubation for mechanical ventilation. An oblique incision of ~1cm was then made ~2mm from the left sternal border, toward the left armpit. The sternohyoid muscles were then slightly spread to visualize the paracardial fat, which is then removed. The fact that the paracardial fat depot is positioned adjacent to the ascending aorta allows for its removal without contact to the heart. After removal of the fat depot 4-0 nylon sutures were applied to chest. When needed for transplant the removed paracardial fat depot was placed on ice while the recipient mouse underwent the just described surgical procedure and the donor depot was positioned in place of the original one. Animals were weaned off ventilator and the breathing tube was removed when respiration resumes a normal pattern. Animals were continuously monitored until they were fully awake and mobile. Total surgery time was approximately 20 minutes. Oral non-steroidal anti-inflammatory drug administration was started 24 hours before surgery and continued for 72 hours of post-operative treatment. Slow-release opioids were also administered the day prior to surgery for 72 hours of continued analgesia. All animals continue to be checked daily as part of post-operative care monitoring. No adverse effects or mortality was observed in paracardial fat removal or transplant surgeries.

Lipid extraction and triglyceride assay: For lipid extraction, ~25mg liquid nitrogen frozen tissues were powderized using a tissue pulverizer (Cole-Parmer Scientific) and then immediately resuspended in 250μL ultrapure water. 1mL of a 2:1 v/v chlorophorm : methanol solution was then added to samples, which were then vortexed, kept at room temperature (RT) for 5 minutes, and then centrifuged at 3000 RPM for 5 minutes. Following centrifugation, the bottom layer was transferred to a new tube and rinsed with 50mM NaCl. Following rinse, samples were centrifuged at max speed for 5 minutes. The bottom layer was again transferred to a new tube, rinsed with 1:1 v/v 0.36M $CaCl_2$: methanol solution and centrifuged at max speed for 5 minutes two times. The remaining final layer was transferred to a new tube and speed vacuumed. Lipid samples were then reconstituted in 100% ethanol and used for triglyceride assay analysis. Triglyceride assays were performed using the Wako Diagnostic's L-Type triglyceride reagents (L-Type Triglyceride M Enzyme Color A (R1) Cat. # 994-02891/992-02892 , Cat. # 990-

02991/998-02992 L-Type Triglyceride M Enzyme Color B (R2), Cat. # 464-01601 Multi-Calibrator Lipid). In brief, a standard curve, 4µL of each sample, and 4µL of a water blank were added into a clear 96-well plate. 90µL of R1 was then added to each well, the samples were mixed at 37˚C for 5 minutes, and plate absorbance was read at 600nm (and 700nm as a reference wavelength). Then, 30µL of R2 was then added to each well, the samples were mixed at 37˚C for 5 minutes, and plate absorbance was again read at 600nm (700nm as a reference wavelength). Final absorbance was calculated by subtracting the first measurements from the second. A calibration curve was then generated by plotting final absorbance against known concentration, and using this curve sample concentrations were calculated according to manufacturer's instructions.

Cardiac magnetic resonance imaging (cMRI): Cardiac MRI imaging was performed using a 9.4 T horizontal-bore imaging system (Bruker BioSpect 90/30US, Bruker BioSpin Co., Ettlingen Germany). Mice were anaesthetized with 2-3% isoflurane mixed with carbogen (95%O_2+5%CO_2; 1liter/min) and maintained with 1–1.5% isoflurane during MR imaging. Physiological parameters such as the ECG, respiration and temperature of each mouse were monitored using a small animal monitoring system (Model 1025, Small Animal Instruments, Stony Brook, NY). The ECG signal was obtained by placing two EKG leads on animal body. A pneumatic pillow was used to monitor the respiration. Each animal was placed on the heated holder, secured and placed at the center of the MRI scanner. After initial TriPilot images, FLASH-cinie short axis images have been obtained over five-seven slices with following acquisition parameters: Field of View (FOV): 2.5 cm, Matrix Size 256×256, Repetition Time/Echo Time TR/TE=8/1.4 ms, NAver=4-6, a Flip Angle of 15°. Each slice was manually traced and analyzed using ImageJ software (NIH, Bethesda) to obtain left ventricle: cardiac output, cardiac volumes and ejection fraction.

Primers for real time quantitative PCR: Primers used were: mouse *Rpl7* (5′-TGGAACCATGGAGGCTGT-3′, 5′- CACAGCGGGAACCTTTTTC-3′); human *Rpl7* (5'-ATGCGCCAACTTCCTCTTT-3', 5'-CAGCTCTGCGAAATTCCTTC-3'); mouse *Adh1* (5'-CAATGCCCAGAACCTCTCCA-3', 5'-TCCAGAACGAAGCAGGTCAA-3'); human *Adh1* (5'- GCTGCTACTGACTGGACGTA-3', 5'- TTTCCCAGAGTGAAGCAGGT-3'); mtDNA (5'-TTG GGT TGT TTG ATC CTG TTT CG -3', 5'- CTT CGC TTT CCA CTT CAT CTT ACC -

3'); nDNA (5'- CAG GAT GCC TCT CTT GCT CT-3', 5'- CGT CTT CCC CTC CAT CGT-3'); mouse *Mfn1* (5'-GCCATCACTGCAATCTTCGG-3', 5'-GAGACAGCACCTCCCCAATG-3'); mouse *Mfn2* (5'-GACGAGCAATGGGAAGAGCA-3', 5'-CATCACACTCACCATGCTGC-3'); mouse *Opa1* (5'-CATCCTGCCCTCAAGCTTCA-3'; 5'-CCTCCAACAGCAGATCCCAG-3'); human *Opa1* (5'-GCGGGATGTGGCGACTAC-3'; 5'-ATTGGGGTCGTTGAAGCTTT-3'); mouse *Aldh1a1* (5'-ATGGATGCTTCAGAGAGGGG-3', 5'-CCCAGCCTGCACAGTACTTT-3'); mouse *Aldh1a2* (5'-ATGGGTGAGTTTGGCTTACG-3', 5'-GGTTGGAGGGAAGGAGAGTC-3'); mouse *Aldh1a3* (5'-GCACCGACTATGGACTCACA-3', 5'- CCCAGACATTTTGAAGCCACC -3'); mouse *Adh4* (5'-TGGACGTTATATTGGGCCGT-3', 5'-CTTCATCAGGTCAATGGCATCA -3'); mouse *Adh5* (5'- GGTGTCAGTGTGGTAGTGGG -3', 5'- GGAGAGATTGCCGGTCACAA -3'); mouse *Adh6a* (5'- CGTCTGTCTGATCGCTGGG -3', 5'-GGAGCTGGTTAAAAGGCAGC-3'); mouse *Adh6b* (5'-CCGGTTCCCAGCTCTCTTTT-3', 5'- TGGGAAAGGCAGTCTATGGG -3'); mouse *Adh7* (5'-CTCCTCCGTCAGCCAAGATG-3', 5'-AGGCAAGGTGTGGGTTATCA-3'); mouse *Rdh1* (5'- CCAGCTCGGAAGTCAAAGAG -3', 5'- GAGAAGGGCATCCACAAGAA -3'); mouse *Rdh10* (5'-CTGCTGGTTCTCTGGGACAT-3', 5'-TTCCCCACGTCACAAGTGTA-3'); mouse *Cyp26a1* (5'-CGGTTCAGCTTCATTCCATT-3', 5'-GTGGGGCTTGTCTTCATTGT-3'); mouse *Cyp26b1* (5'- TTCTCTCTGCCAGTGGACCT -3', 5'- GGTCATCTCCTTGCCATGTT -3'); mouse *Crebp1* (5'-GACTCCAACGCCAACAAGAT-3', 5'- AGGTAAAGGGCTGTCCTGGT -3'); mouse *Pref1* (5'- AGTATGGATTCTGCGAGGCTG-3', 5'- AATTTCCCGTCCCAGCCATC -3'); mouse *Adipoq* (5'- CTATTAGCTCTGCCCGGTCA -3', 5'-GAGCGATACACATAAGCGGC -3'); mouse *Ucp1 (*5'- CGTCCCCTGCCATTTACTGT-3', 5'-ATGATGACGTTCCAGGACCC-3'); mouse *Prdm16* (5'-GAACCAGGCATCCACTCGAA -3', 5'- CGTGTCCTCCTGTGACTTCC -3'); mouse *Bmp7* (5'-AGGGCTGGTTGGTGTTTGAT -3', 5'- AAGGGTTGCTTGTTCTGGGG -3'); mouse *Cebpa* (5'-CCCCACTTGCAGTTCCAGAT-3', 5'-CACCGACTTCTTGGCTTTGC -3'); mouse *Rbp4* (5'-TGAAGTACTGGGGTGTAGCC-3', 5'-TGGGGTCACGAGAAAACACA-3'); mouse *Fabp4* (5'-TTTCCTTCAAACTGGGCGTG -3', 5'- CACCAGCTTGTCACCATCTC -3').

Transcriptomics analysis: A filtering method based on percentage of arrays above noise cutoff was applied to filter out low expression genes. Linear model was employed to detect differentially expressed genes. In order to improve the estimates of variability and statistical tests for differential expression, a variance smoothing method with fully moderated t-statistic was employed for this study. The significance level was adjusted by controlling the mean number of false positives. Principle component analysis (PCA) was used to discriminate samples based on gene expression profiling. The data of all genes were projected onto multiple dimensions (i.e., PC1, PC2, and PC3) for each sample, where PC1, PC2, and PC3 are the first three dimensions with the largest variation of the expression data and they are the linear combinations of all genes' expression.

Metabolomics analysis: We used the NEXERA XR UPLC system (Shimadzu, Columbia, MD, USA), coupled with the Triple Quad 5500 System (AB Sciex, Framingham, MA, USA) to perform hydrophilic interaction liquid chromatography analysis, NEXERA XR UPLC system (Shimadzu, Columbia, MD, USA), coupled with the Triple TOF 6500 System (AB Sciex, Framingham, MA, USA) to perform reversed-phase liquid chromatography analysis, and Agilent 7890B gas chromatograph (Agilent, Palo Alto, CA, USA) interfaced to a Time-of-Flight Pegasus HT Mass Spectrometer (Leco, St. Joseph, MI, USA). The GC system was fitted with a Gerstel temperature-programmed injector, cooled injection system (model CIS 4). An automated liner exchange (ALEX) (Gerstel, Muhlheim an der Ruhr, Germany) was used to eliminate cross-contamination from the sample matrix that was occurring between sample runs. Quality control was performed using metabolite standards mixture and pooled samples. A standard quality control sample containing a mixture of amino and organic acids was injected daily to monitor mass spectrometer response. A pooled quality control sample was obtained by taking an aliquot of the same volume of all samples from the study and injected daily with a batch of analyzed samples to determine the optimal dilution of the batch samples and validate metabolite identification and peak integration.

Metabolite pathway analysis: Metabolomic data was analyzed as previously described(74). For heatmap generation and analysis the web server "heatmapper" was used (http:/heatmapper.ca). For this, a spreadsheet containing a row for each metabolite was generated with columns for each

animal's normalized value of that metabolite. For animals of the same genotype, the columns were assigned the same numerical header value. The analysis allows users to view un-clustered expression data from metabolomics experiments. The z-scores shown are row z-score values. Identified metabolites were subjected to pathway analysis with MetaboAnalyst 4.0, using Metabolite Set Enrichment Analysis (MSEA) module which consists of an enrichment analysis relying on measured levels of metabolites and pathway topology and provides visualization of the identified metabolic pathways. Accession numbers of detected metabolites (HMDB, PubChem, and KEGG Identifiers) were generated, manually inspected, and utilized to map the canonical pathways. MSEA was used to interrogate functional relation, which describes the correlation between compound concentration profiles and clinical outcomes.